Validation of Satellite-Derived Liquid Water Paths Using ARM SGP Microwave Radiometers

M. M. Khaiyer and J. Huang
Analytical Services & Materials, Inc.
Hampton, Virginia

P. Minnis, B. Lin, and W. L. Smith, Jr.
National Aeronautics and Space Administration
Langley Research Center
Hampton, Virginia

A. Fan
Science Applications International Corporation
Hampton, Virginia

A. Rapp
Colorado State University
Fort Collins, Colorado

Introduction

Satellites are useful for monitoring climatological parameters over large domains. They are especially useful for measuring various cloud microphysical and radiative parameters where ground-based instruments are not available. The geostationary operational environmental satellite (GOES) has been used to retrieve cloud and radiative properties over an extended domain centered on the Atmospheric Radiation Measurement (ARM) Southern Great Plains (SGP) Central Facility (CF). One of the microphysical parameters available from the GOES-8 dataset is cloud liquid water path (LWP), which is crucial for linking the atmospheric hydrological and radiative budgets. Preliminary validation of this parameter has been limited to a very few cases of thick stratus during March 2000. To better understand and validate the GOES-derived LWP more completely, this paper compares it with LWP retrievals based on ARM's ground-based microwave radiometers (MWR) at the SGP central and boundary facilities. The comparisons utilize data taken in a variety of cloud conditions during March 2000 to examine the relationships between the GOES-8 and microwave LWP retrievals as related to cloud temperature, cloud type, and viewing angle.

Data and Methodology

The visible infrared solar-infrared split-window technique (VISST) has been used to analyze 4-km data from the 0.65, 3.9, 11, and 12-μm channels of the GOES-8 imager since March 2000 (Minnis et al. 2001). LWP is derived from the retrieved values of effective radius Re and visible optical depth τ_v. The

ARM MWR data were taken at sites B1 (Hillsboro, Oklahoma; 38.31°N, 97.30°W), B4 (Vici, Oklahoma; 36.07°N, 99.20°W), B5 (Morris, Oklahoma; 35.69°N, 95.87°W), and the SCF C1 (Lamont, Oklahoma; 36.61°N, 97.49°W). Two different MWR LWP datasets are used: from the standard ARM retrieval (Liljegren et al. 2001) and from retrieval using the algorithm of Lin et al. (2001). The latter retrieval uses a variety of input data in addition to the MWR measurements. Cloud base height information was obtained from the vaisala ceilometer (VCEIL) data at B1, B4, and B5 and from the active remote sensing of cloud layers (ARSCLs); see Clothiaux et al. 2000) dataset at the CF. Surface pressure and air temperature, as well as temperature and wind direction at cloud base height, were taken from the rapid update cycle 3-hourly model output. The ARM MWR provided 23.8 and 31.4-GHz brightness temperatures at 20-s sampling intervals. These data were averaged to 3-minute intervals. The infrared thermometer (IRT) provided equivalent blackbody temperature of the clouds in the 9.6 μm to 11.5 μm atmospheric window.

The Lin et al. (2001) retrieval algorithm uses the Liebe (1989) model for gaseous absorption. To process the data, water clouds were assumed to be single-layered with cloud tops below 5 km and cloud temperatures greater than 241 K. LWP is retrieved beginning with

$$R_{cld} - R_{clr} = (1 - \exp(-\tau)B(T_{cld})) \quad (1)$$

where R_{cld} is cloudy IRT radiance, R_{clr} is clear-sky IRT radiance (taken from a look-up table), τ is the cloud infrared (IR) optical depth, B is the Planck function, and T_{cld} is cloud temperature. The LWP retrieval scheme iterates between retrieving LWP and column water vapor (CWV) using MWR brightness temperature measurements, estimating T_{cld} from observations using a four-step process. First, an initial estimate of T_{cld} is made using an atmospheric profile calculated from the microwave radiative transfer model (MWRTM) using the ARM LWP, CWV, cloud base height and temperature. Second, the MWRTM simulates the MWR brightness temperature using the ARM values of LWP, CWV, and T_{cld}. LWP and CWV are adjusted until the difference between the simulated and observed MWR brightness temperatures is less than 0.03 K for both the 23.8 and 31.4-GHz channels. Third, the LWP resulting from step 2 is used to recalculate T_{cld}. Finally, steps 2 and 3 are repeated until the change in LWP between consecutive iterations is less than 0.001 mm.

Both the ARM and Lin-derived LWP retrievals were compared to LWP retrieved using the VISST algorithm. The MWR and VISST results were matched using the average for a swath of GOES-8 pixels approximately corresponding to the portions of cloud viewed by the radiometers. The pixels were chosen according to wind speed and direction at VISST-derived cloud base height. Any pixels in that wind direction, within a distance defined by half hour multiplied by wind speed, were chosen. Additionally, only 100% water cloud cases from daytime were used in the LWP comparisons. Values of the MWR LWP were averaged to 30-minute intervals to match the VISST data.

Results

Figure 1 shows a comparison of Lin and VISST LWP including the RMS differences of the Lin retrievals for each half-hour segment. The green line depicts the linear fit to the data; the yellow denotes the line of one-to-one correlation. VISST consistently overestimates the LWP compared to the Lin

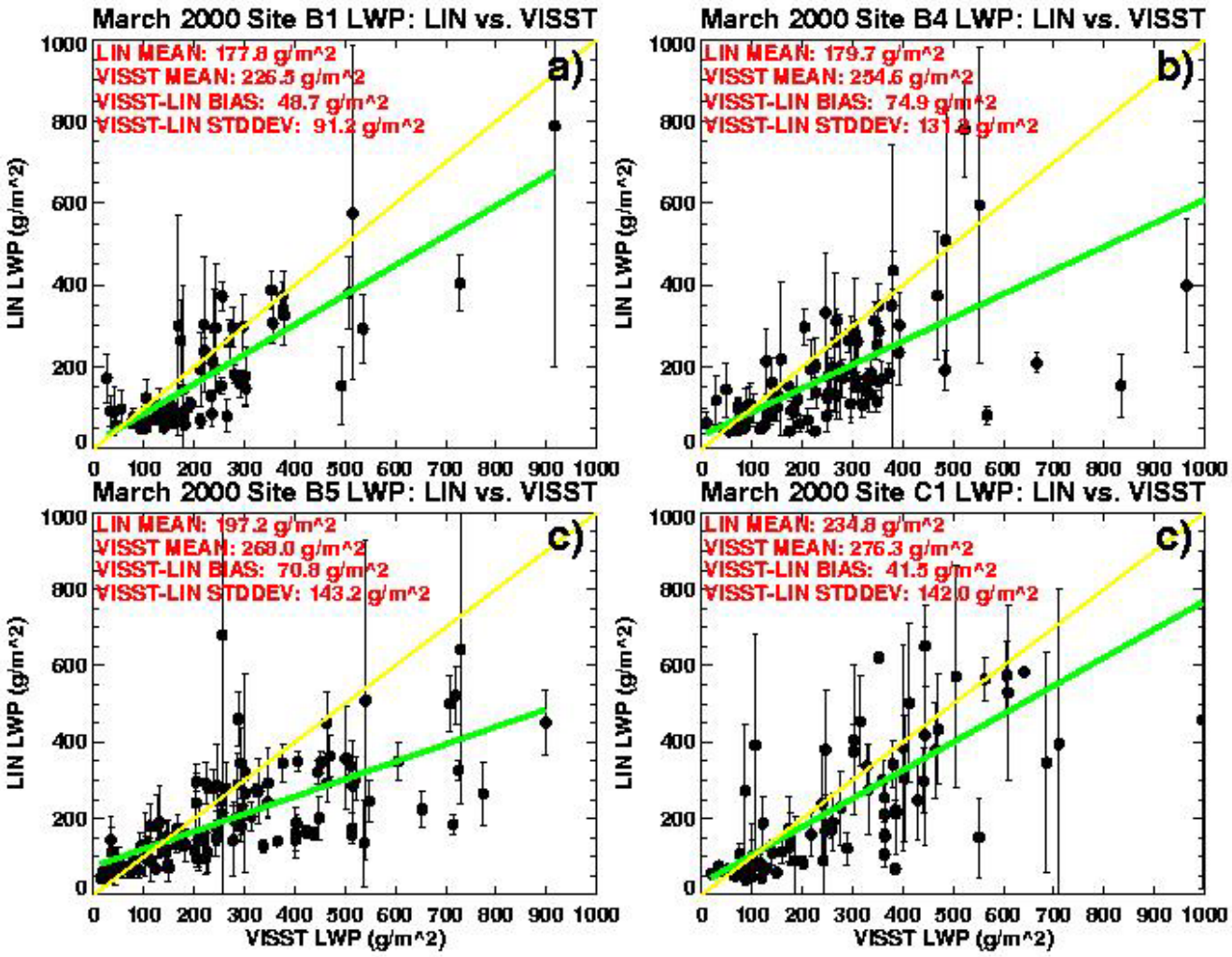

Figure 1. Comparison of half-hour averages of Lin-derived LWP vs. VISST-derived LWP for a) site B1, b) site B4, c) site B5, and d) site C1. The yellow line denotes one-to-one correlation, and the green line the best fit to the data. Error bars indicate the RMS differences for the half-hour averages of Lin-derived LWP.

method with biases of 48.7 (B1), 74.9 (B4), 70.8 (B5), and 41.5 (C1) gm^{-2}. Figure 2 shows a scatterplot of the ARM and Lin-derived LWP results. The Lin retrieval is smaller than the ARM LWP by 46.3 (B1), 42.3 (B4), 37.0 (B5), and 79.8 (C1) gm^{-2}. Figure 3 shows the comparison of the ARM and VISST LWP. VISST overpredicts the ARM LWP, but by a smaller amount than it overpredicts the Lin LWP: mean biases exist of 8.4 (B1), 34.3 (B4), 37.0 (B5), and 0.7 (C1) gm^{-2}. For all sites combined, the half-hourly LWP derived by VISST overpredicted ARM with a bias of 22.6 gm^{-2},VISST-derived LWP had a bias of 61.3 gm^{-2} over Lin-derived LWP; and the 3 minute averaged LWP derived by Lin underpredicted ARM by 41.8 gm^{-2}.

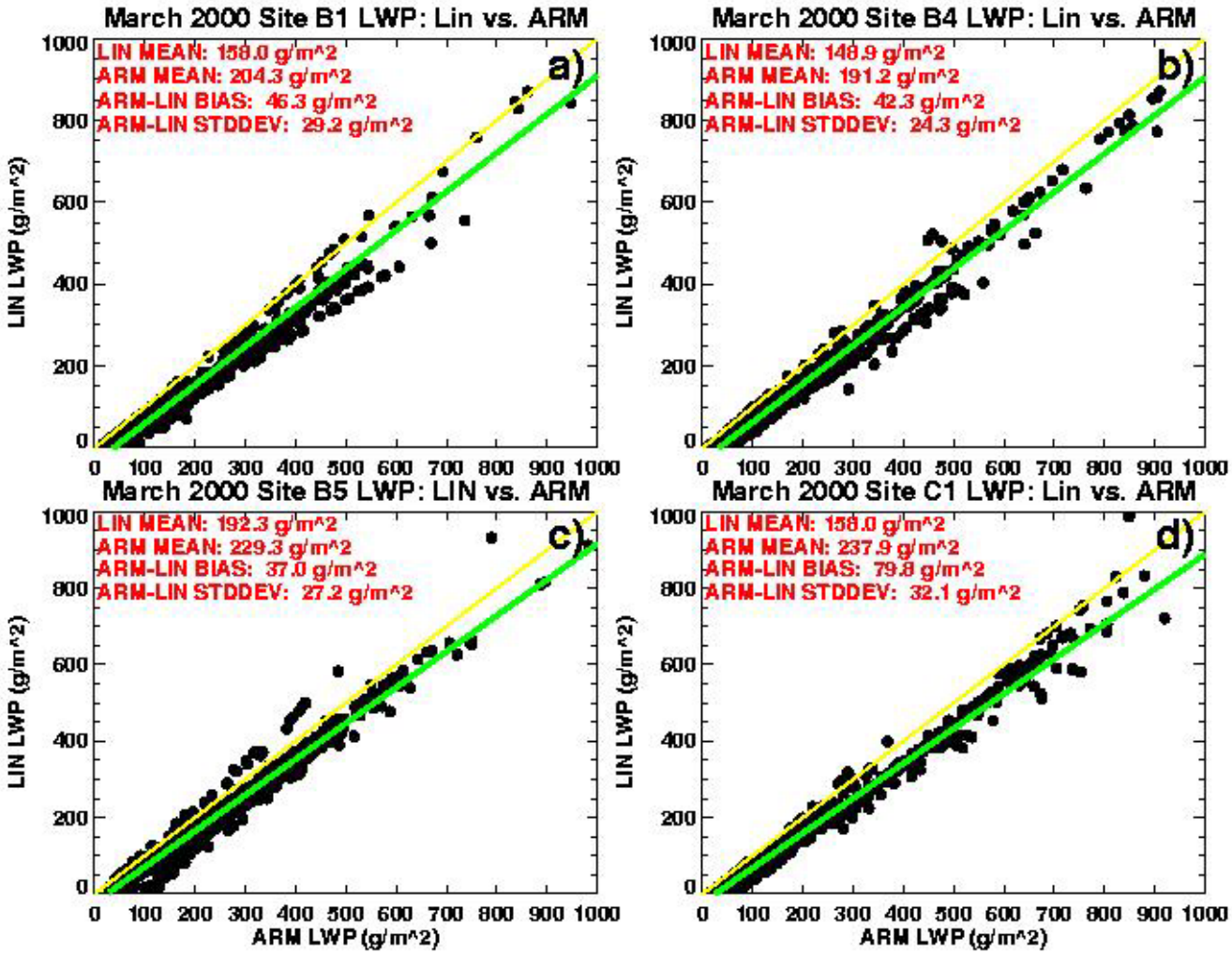

Figure 2. Comparison of 3 minute averaged Lin and ARM-derived LWP for all 4 sites.

Discussion

The ARM and Lin LWP's appear to differ by an almost constant value. To determine the cause for this, differences between the two for clear-sky cases must be examined for any inherent bias that may arise because of differences in calibration of the algorithms. Such differences should be most evident in the clear-sky cases. Figure 4 shows cases defined as mostly clear cases by VISST, although it is apparent that some clouds are present in the results. For all 4 sites, the difference between the Lin and ARM LWP's when ARM LWP = 0 is –18.1 gm^{-2}. Because the ARM data are continuously calibrated using any available clear sky data, the zero point for the ARM technique should be more accurate than the Lin zero point since the latter has not yet been calibrated. Thus, approximately 18 gm^{-2} of the VISST-Lin bias may be due to the lack of calibration in the Lin method.

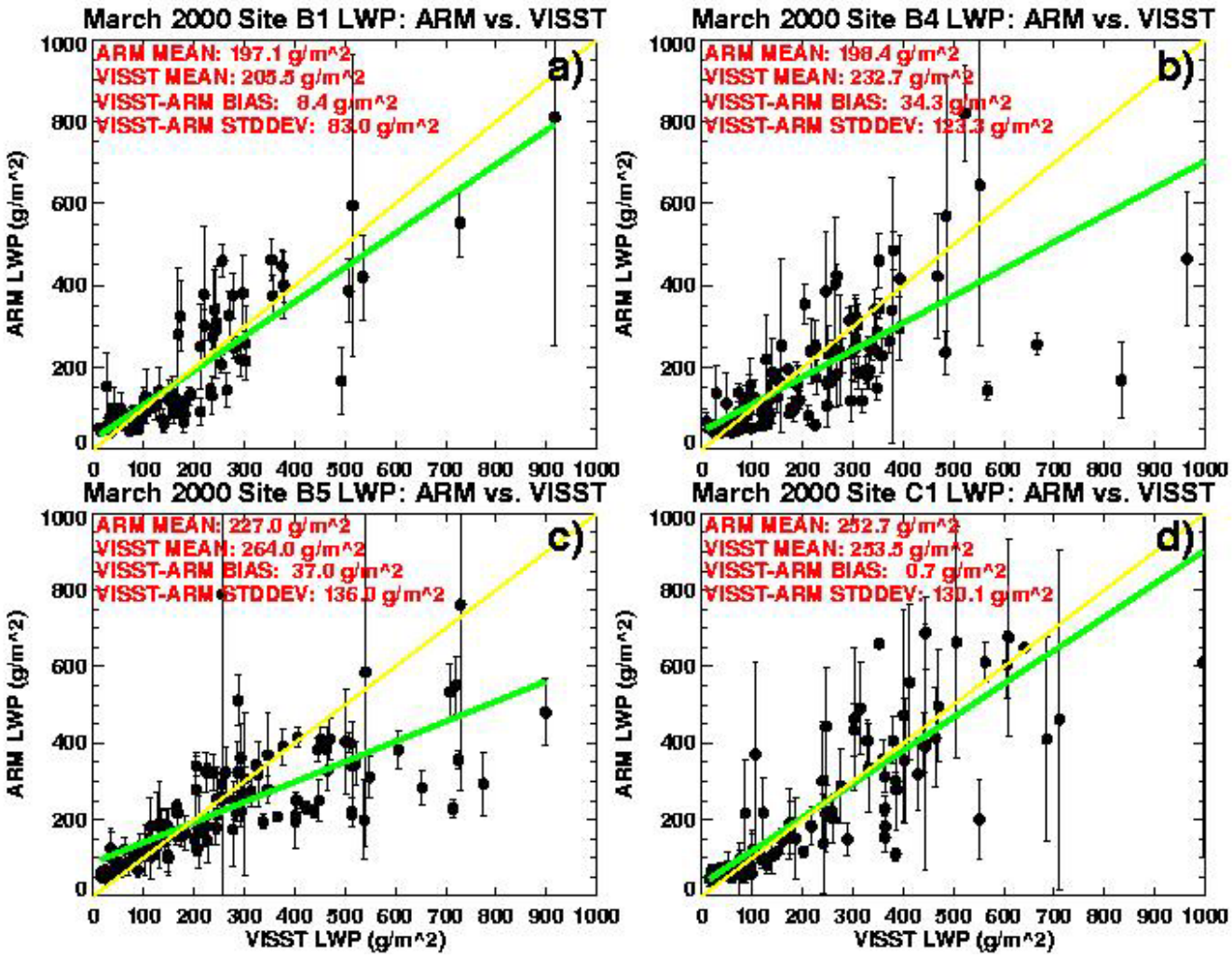

Figure 3. Comparison of half-hour averages of ARM vs. VISST-derived LWP for all four sites. Error bars show the RMS differences for the half-hour averages of ARM-derived LWP.

Differences in LWP between VISST and Lin and between VISST and ARM increase with increasing LWP. Part of this effect may be due to an overestimate of Re in the VISST method for clouds with larger optical depths. The VISST retrieval of Re corresponds to the mean value for a layer at the top of the cloud that may correspond to a value of τ_v <10. For clouds with larger optical depths, the retrieved value of Re can be too large because the droplets in the lower part of the cloud are usually much smaller than those at the top. Thus, the overestimate of LWP should increase with τ_v when the droplet radius increase with height in the cloud. Further adding to the overestimate of LWP, optical depth is larger for larger effective radii at a given reflectance. To account for this effect, the results of Dong et al. (2002) were used to determine the variation of the Re difference with τ_v and estimate a correction for the thickness effect on LWP. Figure 5 shows the ARM LWP compared to VISST LWP after correction of the latter using the formula

$$\text{LWPnew} = \text{LWP}(\text{I} - \text{F}) \qquad (2)$$

where

$$F = (0.000000157\,\tau_v^3 - 0.00004719\,\tau_v^2 + 0.00501574\,\tau_v - 0.028204)\,R_e/12 \quad (3)$$

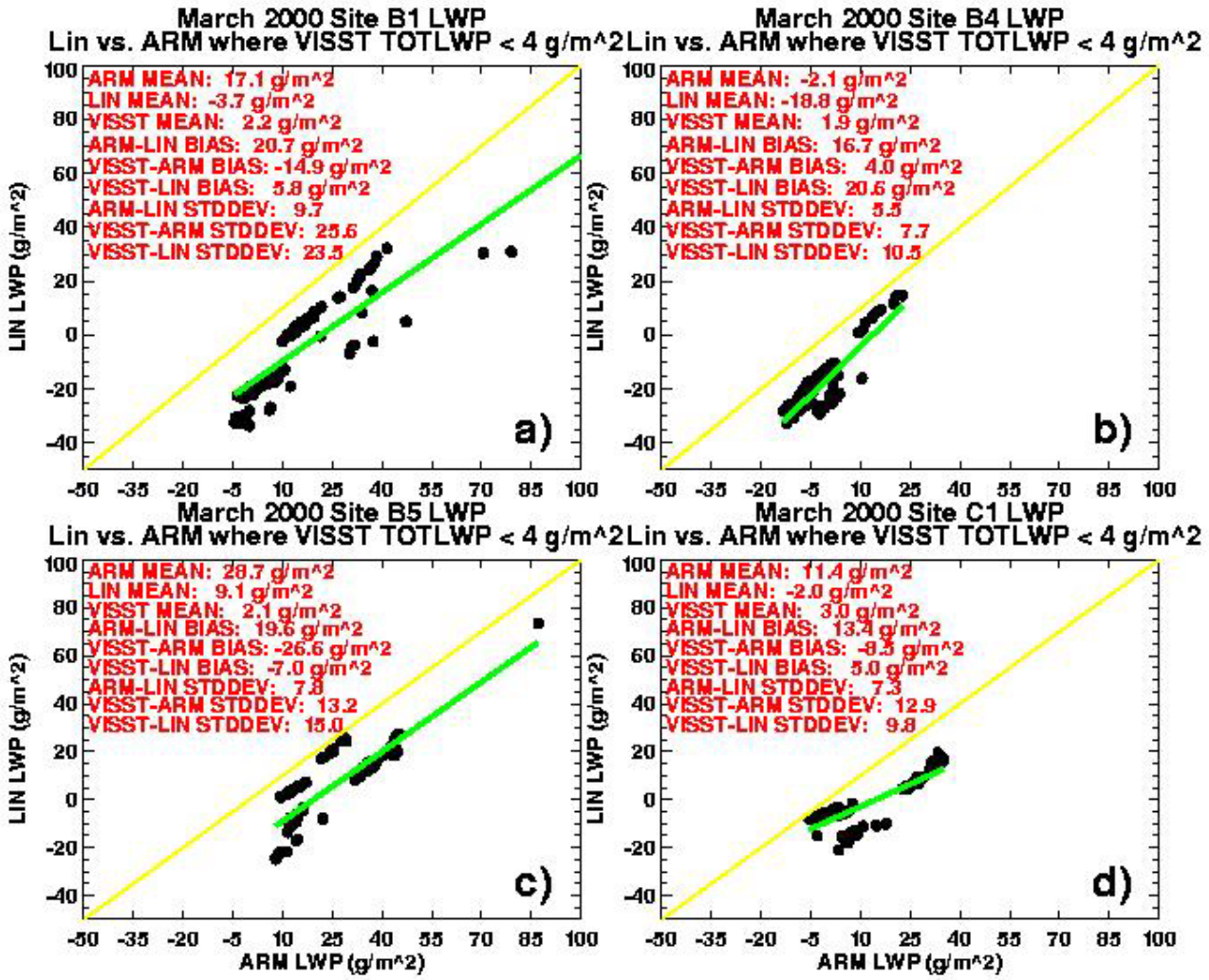

Figure 4. Comparison of Lin and ARM-derived LWP for cases where VISST-derived. Total LWP is less than 4 g/m^2. Total TWP is defined as LWP multiplied by water cloud percentage.

was determined from the Dong et al. (2000) results. The linear fits to the corrected data (green line) in Figure 5 generally show better agreement than those in Figure 3, except over the SCF where the correction was developed. The combined bias for all four sites of 22.6 gm^{-2} decreased to –0.3 gm^{-2}. The standard deviation of the differences is 116.4 g m^{-2} compared to 122.8 gm^{-2} for the uncorrected case. Similarly, the mean difference between the VISST and Lin LWP (not shown) is cut in half from 61.3 gm^{-2} to 31 gm^{-2}.

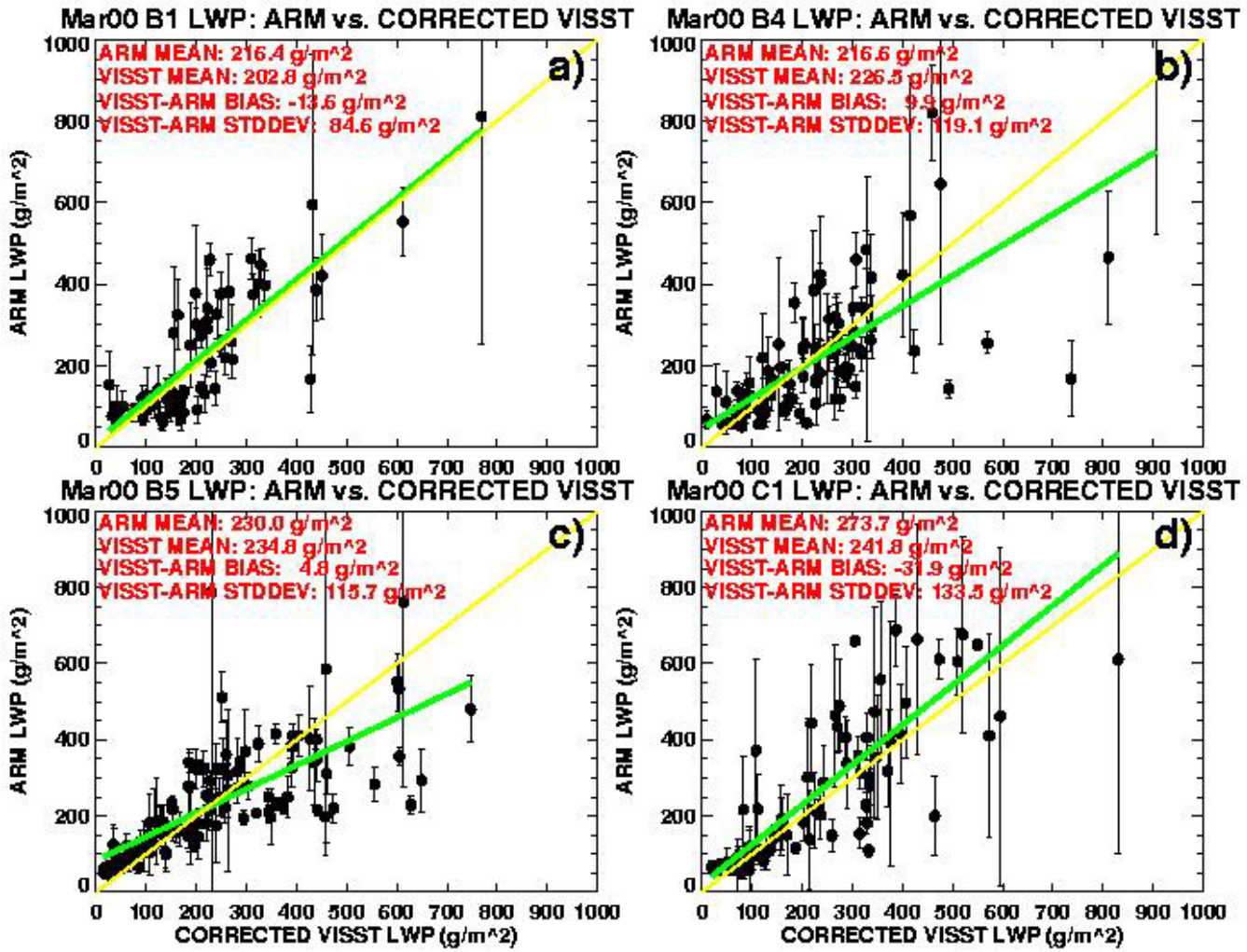

Figure 5. Comparison of ARM and VISST-derived corrected LWP for all 4 sites. Error bars denote the RMS differences for the half-hour averages of ARM-derived LWP.

Other reasons for the discrepancies may be due to inadequate modeling of the reflectance fields since a plane-parallel model is used for the VISST and most clouds are not flat sheets. Bumps on cloud tops and other vertical structure in real clouds cause more reflection in the backscattering direction than in the plane-parallel radiative transfer model. Similarly, because of partial shadowing by the same vertical structure, less radiation is reflected in the cross-scattering direction than expected with the plane parallel model. Also, the absorption models used by Lin and ARM differ for the supercooled clouds and may, therefore, introduce additional sources of discrepancies in the results. Figure 6 shows the variations of the cloud properties as functions of the scattering angle and cloud temperature. Figures 6a and b show averaged τ_v, Re, and ARM LWP for 10° scattering angle bins, and 10° cloud temperature bins. The corresponding average differences between VISST, corrected VISST, ARM, and Lin LWP values, are shown in Figures 6c and 6d.

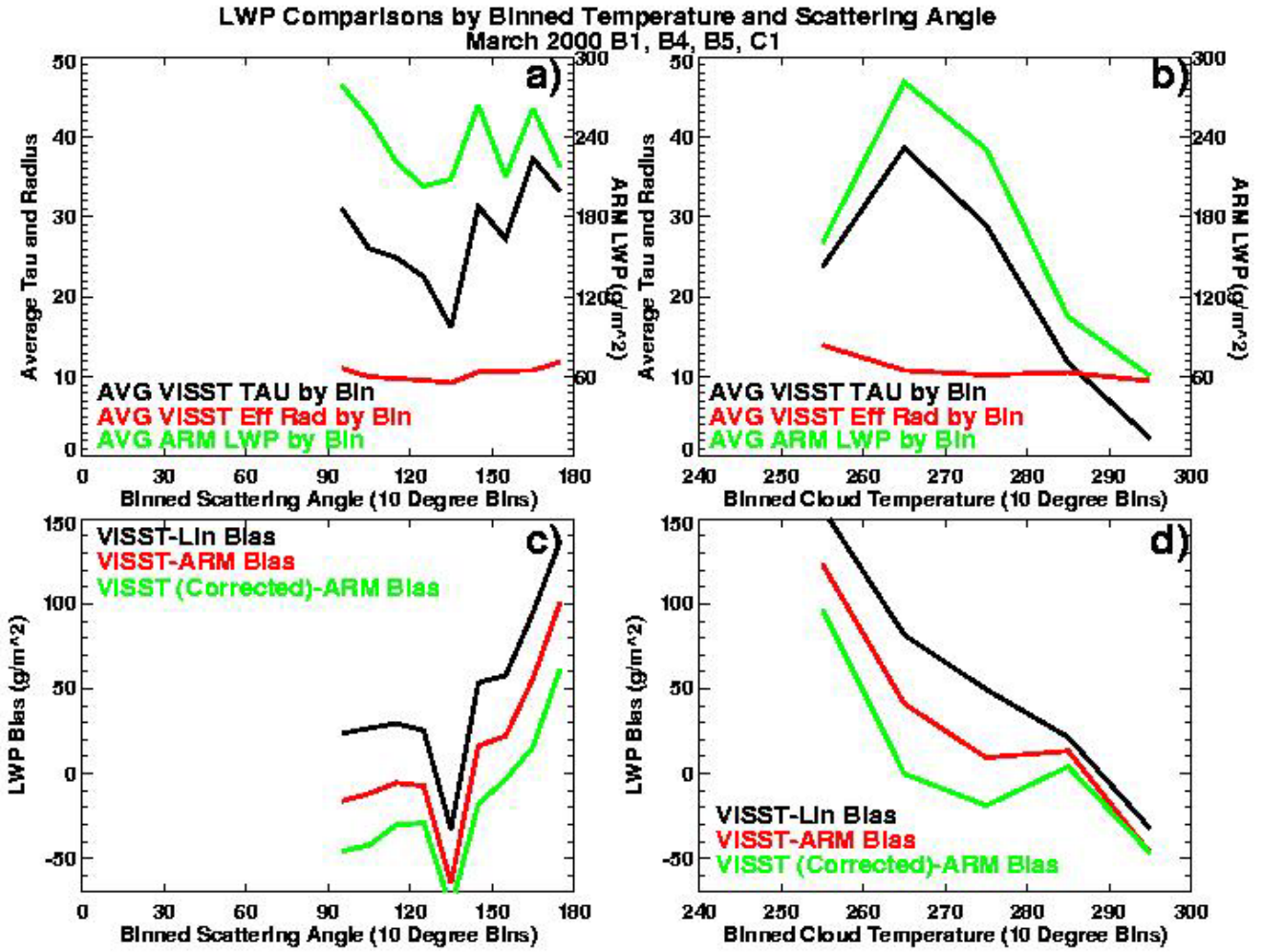

Figure 6. Comparisons by binned temperature (10 degree K bins) and scattering angle (10 degree bins) of: a)averaged VISST-derived optical depth (black), effective radius (red), and LWP (green) per scattering angle bin; b) same as a) but for cloud temperature bins; c) average LWP biases for VISST-Lin (black), VISST-ARM (red) and corrected VISST-ARM per scattering angle bin; d) same as c) but for cloud temperature bins.

The average value of Re varies with scattering angle by only 2 μm (Figure 6a), but is generally flat as a function of cloud temperature (Figure 6b). The ARM LWP and τ_v tend to converge with increasing scattering angle (Figure 6a) resulting in the bias increasing with scattering angle (Figure 6c). Part of this dependence may be the result of 3-D effects in clouds that are not taken into account by the plane-parallel models used to interpret the reflected radiances. Thus, the trend in the biases in Figure 6c may be explained in part by 3-D effects. The undulations in the curves may be a result of sampling or to interpolation errors in the VISST models. These differences warrant additional study.

Cloud optical depth and ARM LWP tend to diverge with increasing temperature (Figure 6b), but this divergence is compensated in part by the Re effect (Figure 6d). Figure 6d shows that the two differences diverge with decreasing cloud temperature. Note that the results at 255 K and 295K are not

significant since there are only 9 samples at 255K and 1 sample at 295K, compared to 139, 165, and 42 samples in the remaining temperature ranges. The bias between the Lin and ARM LWPs for warm clouds (T > 280K) is nearly the same as the bias for clear-sky conditions indicating that the two methods agree for those cases. The two MWR techniques differ in their treatment of supercooled clouds. This difference is reflected in the divergence of the two curves in Figure 6d. The Lin method was shown to more accurately reproduce in situ cloud LWP measurements in supercooled clouds in the Arctic than the ARM approach (Lin et al. 2001) and, therefore, should provide the better assessment of the LWP in the SGP supercooled clouds. The in situ data from the March 2000 cloud IOP included only two supercooled cloud cases with cloud-top temperatures at 271 K, a degree of supercooling that is insufficient to illuminate the differences between the Lin and ARM retrievals. Additional in situ data are needed to determine the MWR retrieval accuracies over the SGP domain.

Concluding Remarks

The mean values of ARM and Lin LWP values will be compared again after the Lin method is calibrated using available clear-sky data. The new results should provide definitive differences between the two methods that will need further resolution using other instrumentation such as in situ, radar, or solar radiometer datasets. Also, further comparisons using data from throughout 2000 will be made.

Additional study of the effect of vertically varying droplet radius is needed to refine any correction methods. The VISST methodology should be corrected to account for the vertical variation of droplet size and the resulting change in R_e and optical depth. The results will then be compared with the new values from the MWR datasets. A new high-angular resolution reflectance lookup table will be incorporated into VISST to reduce interpolation errors with the aim of reducing any remaining model-dependent angular biases and scatter in the satellite retrievals. The changes should lead to improvements in the satellite retrievals and enhance their utility for understanding the radiation and hydrological cycles over the ARM domains.

Corresponding Author

Mandana Khaiyer, m.m.khaiyer@larc.nasa.gov, (757) 827-4642

Acknowledgments

The ARSCL, VCEIL, GOES-8 data, and MWR data were obtained from the Atmospheric Radiation Measurement Program sponsored by the U.S. Department of Energy, Office of Science, Office of Biological and Environmental Research, Environmental Sciences Division. Periods of GOES-8 data, as well as the 3 hourly RUC data used in the retrievals, were obtained from the Space Science and Engineering Center at University of Wisconsin-Madison. This research was sponsored by ITF No. 214216-A-Q1 from Pacific Northwest National Laboratory.

References

Clothiaux, E. E., T. P. Ackerman, G. G. Mace, K. P. Moran, R. T. Marchand, M. Miller, and B. E. Martner, 2000: Objective determination of cloud heights and radar reflectivities using a combination of active remote sensors at the ARM CART sites. *J. Appl. Meteorol.*, **39**, 645-665.

Dong, X., P. Minnis, T. P. Ackerman, E. E. Clothiaux, G. G. Mace, R. N. Long, and J. C. Liljegren, 2000: A 25-month database of stratus cloud properties generated from ground-based measurements at the ARM SGP Site. *J. Geophys. Res.*, **105**, 4529-4537.

Liebe, H., 1989: MPM—An atmospheric millimeter-wave propagation model. *Int. J. Infrared and Millimeter Waves*, **10**, 631-650.

Liljegren, J. C., 1999: Automatic self-calibration of ARM microwave radiometers. *Microwave Radiometry and Remote Sensing of the Earth's Surface and Atmosphere*, P. Pampaloni and S. Paloscia, Eds., pp. 433-443, VSP Press.

Liljegren, J., E. Clothiaux, G. Mace, S. Kato, and X. Dong, 2001: A new retrieval for cloud liquid water path using a ground-based microwave radiometer and measurements of cloud temperature. *J. Geophys. Res.*, **106**, 14,485-14,500.

Lin, B., P. Minnis, A. Fan, J. A. Curry, and H. Gerber, 2001: Comparison of cloud liquid water paths derived from in situ and microwave radiometer data taken during the SHEBA/FIREACE. *Geophys. Res. Lett.*, **28**, 975-978.

Minnis, P., W. L. Smith, Jr., D. F. Young, L. Nguyen, A. D. Rapp, P. W. Heck, S. Sun-Mack, Q. Trepte, and Y. Chen, 2001: A near-real time method for deriving cloud and radiation properties from satellites for weather and climate studies. In *Proc. AMS 11th Conf. Satellite Meteorology and Oceanography*, October 15-18, 2001, pp. 477-480, Madison, Wisconsin.